32% Efficient Thickness Optimized Lead-Free $CsSnI_3$ Perovskite Solar Cells with TiO_2 Electron Transport Layer

Nabanita Mondal[1*], Debamita Roy[2] and Abhijit Biswas[1]

[1]Department of Radio Physics and Electronics, University of Calcutta,
[1]92, Acharya Prafulla Chandra Road, Kolkata, West Bengal, India.
[2]Heritage Institute of Technology,
[2]Chowbaga Road, Kolkata, West Bengal, India
Corresponding Author: nabanitamondal54@gmail.com

ABSTRACT

The increasing demand for eco-friendly and high-efficiency photovoltaic technologies has intensified potential research on lead-free perovskite solar cells. However, in planar and tandem perovskite material based solar cells it is still a challenge to maintain proper band alignment between successive layers along with maintaining lower rate of charge carrier recombination yielding high photo conversion efficiency (PCE). This paper proposes an environment friendly lead free ITO/TiO_2/$CsSnI_3$/PEDOT:PSS/Al-based planar solar cell designed for efficient capture of the solar radiation. $CsSnI_3$ acts as the narrow-bandgap active absorber layer, enabling effective photon absorption and generation of electron–hole pairs. The layer below the front electrode serves as an electron transport layer (ETL) whereas the layer above the back contact works as hole transport layer (HTL), and the materials are selected based on favorable band alignment with the absorber layer. The layers above absorber are chosen to function as window layer for the incident solar irradiation. The energy band diagram is also presented to illustrate carrier transport and reduced recombination losses across the ETL and HTL. The simulation study is carried out using Ansys Lumerical implementing FDTD method along with using it's CHARGE solver module which suggest that a perovskite layer thickness of 300 nm yields the optimal performance, achieving a photo conversion efficiency (PCE) of 32.1%, along with a short-circuit current density (J_{sc}) of 42.71 mA/cm², an open-circuit voltage (V_{oc}) of 0.91 V, and a fill factor (FF) of 82.4%. The obtained PCE is among the highest values reported recently for perovskite lead-free planar solar cells.

Keywords: ETL, HTL, PCE, Perovskite based solar cells, photovoltaic (PV), figures of merit (FOM).

I. INTRODUCTION

Global demand for eco-friendly renewable energy has been accelerated in recent years. Out of all solar photovoltaics has drawn significant attention due to its capability of directly converting sunlight into electricity without causing environmental pollution. Perovskite is well known for its high absorption co-efficient compared to traditional silicon based solar cells. A thin film absorbing material is enough to absorb the solar spectrum, leading to low-cost fabrication. Band gap tenability by varying mole fraction of the composition of Perovskite material allows it optimization for wide range of Perovskite solar cell applications. Longer carrier diffusion length of Perovskite material results better charge separation causing higher efficiency.

In earlier works, *Bankura and Biswas* [1] proposed methods like insertion of metallic nanostructures to enhance PCE of lead based wide band gap solar cells and reported a PCE of 32.80%. *Iqbal and co-workers* [2] used $CsPbI_3$ as an absorbing layer and achieved PCE of 14.8% experimentally [2]. *Bala et al.* [3] investigated effect of various ETL and HTL on Solar parameters with lead free $CsSn_{0.5}Ge_{0.5}I_3$ as active material and reported PCE of 23.47%. *Fatima and others* [4] performed simulation study on $CsSnI_3$ material based planar perovskite solar cell (PSC) and achieved high PCE of 31.09%. *Zhou et al.* [5] reported a highly stable perovskite solar cell with PCE of 26.41% experimentally. *Bankura and Biswas* [6] developed analytical model of 2D RP perovskite and after optimization reported PCE of 23.61%. *Tian et al.* [7] introduced defect passivation mechanism and reported an increment of PCE from 17.94% to 20.20% by reduction in surface potential fluctuation and improved charge extraction through interfacial dipole formation. *Bhattarai and collaborators* [8]., with a novel bio-synthesized ZnO-NP ETL to reduce the fabrication cost, reported a PCE of 26.32%. *Chen et al.* [9] reported a PCE of 23.87% with Lewis base strategy for crystallization control and buried interface passivation. *Zhang and co-workers* [10], reported a PCE of 24.13% by introducing a non-covalent binding agent to target the open metal sites for synchronized crystallization kinetics for the homogeneous Pb-Sn alloy to improve the film quality of the Pb-Sn based perovskite materials. *Bankura and Biswas* [11] investigated and optimized lead free two-dimensional $Cs_3Sb_2I_9$ perovskite solar cell and reported an PCE of 17.91% with a declination of 0.06% at elevated temperatures, showing thermal stability of the device. Nath and Biswas [12] reported

ISBN: 978-81-985770-0-9

PCE of 36.3% by engineering the absorber perovskite material with a tri-layer two-dimensional design.

Despite of significant research in this domain challenges are still there to achieve high PCE. The main objective of this work is implementation of an environmentally friendly lead free, $CsSnI_3$ based ITO/TiO_2/$CsSnI_3$/ PEDOT:PSS /Al solar cell considering n–i–p structure, for efficient utilization of the incident solar spectrum. The proposed device is simulated using the FDTD and CHARGE solver modules of the Lumerical simulation platform. The result highlights that the PV performance can be improved manifold with appropriate choice of ETL as well as HTL considering optimum thickness of narrow bandgap $CsSnI_3$ absorber layer.

II. DEVICE STRUCTURE AND SIMULATION METHODOLOGY

Fig. 1(a) shows the schematic diagram of ITO/TiO_2/$CsSnI_3$/PEDOT: PSS/Al PSC structure with ITO as the transparent front electrode, TiO_2 as the ETL, $CsSnI_3$ serving as lead-free narrow bandgap active absorber layer, PEDOT:PSS as the HTL and aluminum as the back electrode. Fig. 1 (b) shows the unit cell structure of the proposed device simulated under FDTD Lumerical environment in the x-z plane. FDTD module intakes real and imaginary part of refractive index over the entire range of solar spectrum either from in-build models or by user defined material imports for each layer. Periodic

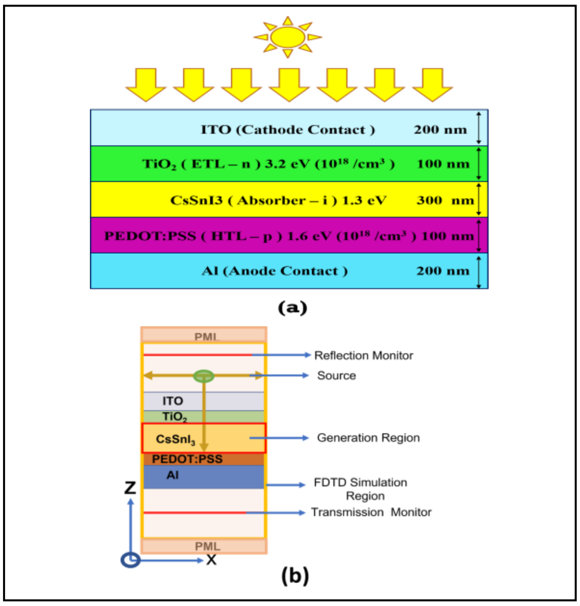

Fig. 1. Device structure of the proposed (a) ITO/TiO_2 /$CsSnI_3$/ PEDOT:PSS /Al solar cell, and (b) unit cell of the solar cell simulated under FDTD Lumerical suite viewed in the x-z plane.

boundary conditions are employed in both x and y directions, while in z direction perfectly matched layer (PML) boundary condition is used to eliminate back reflection of EM waves at the boundaries. AM1.5G solar spectrum is incorporated as the plane wave source with wavelengths ranging from 300 to 1600 nm with the injection axis along z direction backwards.

The optical response of the proposed device is analyzed by the incorporation of the complex refractive index (n-k) profiles for the entire wavelength range of the incident solar spectrum that can be absorbed by individual layers in tandem PSC architecture. The corresponding n-k profiles have been found from literature [[1],[13]]. Finite-Difference Time-Domain (FDTD) method is employed to solve Maxwell's equations numerically by discretizing 3-D device structure into grids and to calculate electric and magnetic fields step by step in time [14]. The photo generation rate profile obtained from FDTD method is incorporated into CHARGE Solver module for further calculation of the electrical responses of the device. All the material parameters and charge carrier transport parameters needed for the simulation study are incorporated in this module. Consequently, key optical responses—such as transmittance, absorptance, and reflectance—can be efficiently evaluated. Using frequency domain power monitors, reflectance and transmittance profiles are obtained and hence absorptance profile is calculated using equation 1 [1].

$$A(\lambda) = 1 - R(\lambda) - T(\lambda), \quad (1)$$

where $R(\lambda)$ is the reflectance and $T(\lambda)$ is the transmittance with wavelength λ.

Lumeical CHARGE solver module solves Poisson's equation coupled with drift–diffusion transport equations by computing the distribution of electric potential and carrier concentrations [15]. Photo voltaic parameters such as V_{oc}, J_{sc}, FF and PCE of the solar cell are thereby evaluated.
FF and PCE (η) are calculated as

$$FF = \frac{V_m \times J_m}{V_{oc} \times J_{sc}} \quad (2)$$

$$\eta = \frac{J_{sc} \times V_{oc} \times FF}{P_{in}}, \quad (3)$$

Where V_m and J_m are the voltage and current density at the maximum power point. J_{sc} is the short circuit current density, V_{oc} is the open circuit voltage, FF is the fill factor and P_{in} is the incident power.

III. MODEL VALIDATION

In order to validate our simulation methodology, a previously reported experimental solar-cell (SC) structure comprising ITO/ TiO_2/ $CsPbI_3$/ Spiro-OMeTAD/ Al is simulated [2] using Lumerical FDFD and CHARGE solver modules. The material

ISBN: 978-81-985770-0-9

and transport parameters for each layer of the device are listed in Table I obtained from well-established literature source [1].

A comparison of simulated and experimental current density vs. voltage characteristics along with extracted solar cell photovoltaic parameters are presented in Fig. 2. The photo-voltaic parameters J_{sc}, V_{oc}, FF, PCE are compared with experimental results to ensure the simulation accuracy. A maximum deviation of 3.5% is observed in PCE. The obtained result confirms the validity of the parameters enlisted and also the selected boundary conditions. The agreement between the simulated results and experimental data ensures the reliability of our simulation framework.

IV. RESULTS AND DISCUSSION

Having validated our simulation framework, we employ this methodology to simulate the optical and electrical behavior of the proposed solar cell consisting of ITO/TiO_2/$CsSnI_3$/PEDOT:PSS/Al structure and to the extract of the photo-voltaic parameters of the device. Here $CsSnI_3$ is the lead free eco-friendly narrow bandgap inorganic perovskite absorbing layer with a band gap 1.3 eV corresponding to cut-off wavelength of 954 nm, which essentially captures the entire visible range along with the infra-red part of the solar spectrum. Another important factor is the transmittance of the layers positioned above the absorber, namely the front electrode and the ETL in the n–i–p configuration. Indium tin oxide (ITO) is employed as the transparent front electrode, while TiO_2 is used as the ETL due to its high optical transmittance—approximately 90% across the visible spectrum and extending into the infrared region [16]. In practice, TiO_2 functions as a window layer for $CsSnI_3$, allowing incident light to efficiently reach the absorber, where photo-generation occurs.

Fig. 3. Portrays absorption spectra of the device as a function of wavelength ranging 300 - 1000 nm with three different thickness values of the absorbing layer from 250 nm to 350 nm with a step of 50 nm. After successful

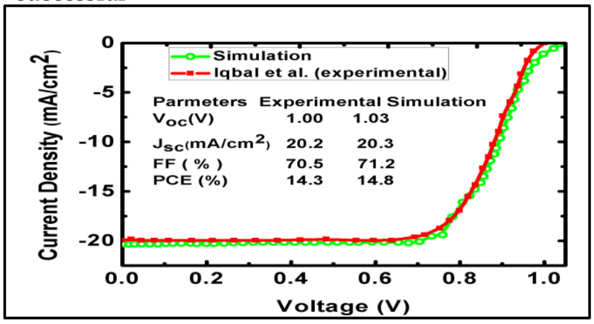

Fig. 2. Comparison of the experimental and simulated J-V characteristics and photovoltaic parameters for ITO/TiO_2/$CsPbI_3$/ Spiro-OMeTAD/Al solar cell.

TABLE I

MATERIAL AND TRANSPORT PARAMETERS OF VARIOUS MATERIALS USED IN THE SOLAR CELL FOR MODEL VALIDATION

Sl. No.	Parameters	Spiro-OMeTAD [1]	$CsPbI_3$ [1]	TiO_2 [1]	ITO [1]
1.	Thickness (nm)	100	300	100	200
2.	Band gap (eV)	3	1.73	3.2	3.5
3.	Work Function (eV)	3.4	3.95	4	4
4.	Relative permittivity (ε_r)	3	6	9	9
5.	Effective mass of electrons ($1/m_0$)	0.04	0.2	0.46	0.3
6.	Effective mass of holes ($1/m_0$)	0.56	0.25	0.14	0.4
7.	Electron mobility(μ_e) (cm^2/V-s)	0.045	16	20	20
8.	Hole Mobility(μ_h) (cm^2/V-s)	0.045	16	10	10
9.	Uniform donor density (cm^{-3}) (N_D) $\times 10^{15}$	0	1.0	10^3	10^5
10.	Uniform acceptor density (cm^{-3}) (N_A) $\times 10^{15}$	10^3	0	0	0
11.	Radiative recombination co-efficient (cm^3/s)	10^{-9}	10^{-9}	10^{-9}	10^{-9}

Insertion of the n-k data for each layer of the proposed planer PSC [[1],[13]], the transmission and reflection profiles are obtained from the simulation results and the absorption curve with wavelength is calculated using (1). From the absorption profile it is clear that due to application of narrow bandgap material $CsSnI_3$, the absorptance spectra improves at higher wavelength regime near the 954 nm cut-off wavelength range and is maintained close to unity which boosts photo carrier generation. The sharp peaks in the lower wavelength regime of absorptance spectra are due to generation of some distinct resonant modes. Also the sharp fall in the absorption profile is not below 50% within a small spectral range qualifies the excellent absorption quality of the perovskite material. Table II enlists the material and transport parameters of individual materials used in the CHARGE module of Lumerical suite for the electrical analysis of the proposed device [[3]-[5]]. Surface recombination velocity (SRV) of 10^4 cm/s is maintained at all the interfaces. The photo generation rate profile obtained from FDTD analys

ISBN: 978-81-985770-0-9

is is imported into the absorber layer in CHARGE solver module for further electrical performance analysis. Fig. 4. Illustrates the energy band diagram of the proposed device, obtained from the CHARGE module. The CsSnI3 absorber of band gap 1.3 eV efficiently captures the solar spectrum, generating electron–hole pairs. The photo-generated holes are transported toward the PEDOT:PSS HTL of band gap 1.6 eV with negligible valence-band offset, facilitating efficient hole extraction. Meanwhile, electrons move toward the TiO2 electron ETL with a band gap of 3.2 eV, encountering only a small conduction-band offset, which still allows effective electron collection. Furthermore, the band alignment suppresses reverse movement of carriers. A significant offset between the valence band of the absorber and the ETL blocks hole transport into the ETL, thereby reducing recombination losses. Similarly, the conduction-band offset between the HTL and the absorber restricts electron leakage toward the HTL. As a result, the probability of carrier recombination within the device is minimized. Fig 5(a) depicts current density – voltage characteristics of the device and Fig. 5(b) potrays power-volatge chracteristics of the proposed device for the for five different absorber layer thicknesses starting from 250 nm to 350 nm with a step of 25nm. Table III summerises the corresponding PV FOMs. The optimized Jsc is obtained as 42.71 mA/cm² with Voc of 0.91V, FF of 82% along with a PCE of 32.1% for an absorber thickness of 300 nm. Although the absorption profile remains nearly similar the observed variation arises from the interplay between optical absorption and charge transport. A small

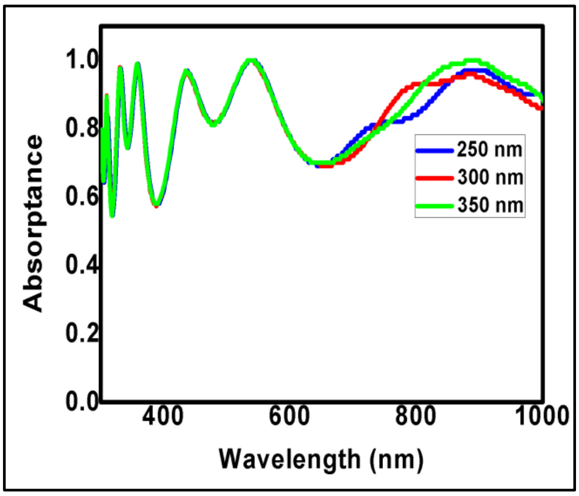

Fig. 3. Simulated absorptance profile of the ITO/TiO2/CsSnI3 /PEDOT:PSS solar cell device for different thickness values

TABLE II
MATERIAL AND TRANSPORT PARAMETERS OF VARIOUS MATERIALS USED IN THE PROPOSED SOLAR CELL

Sl. No.	Parameters	PEDOT:PSS [3]	$CsSnI_3$ [[4]-[5]]
1.	Thickness (nm)	100	300
2.	Band gap (eV)	1.6	1.3
3.	Work Function (eV)	3.4	9.93
4.	Relative permittivity (ε_r)	3	3
5.	Effective mass of electrons ($1/m_0$)	0.3	0.06
6.	Effective mass of holes ($1/m_0$)	0.4	0.03
7.	Electron mobility(μ_e) (cm^2/V-s)	0.045	1500
8.	Hole Mobility(μ_h) (cm^2/V-s)	0.045	585
9.	Uniform donor density (cm^{-3}) (N_D) × 10^{15}	0	1.0
10.	Uniform acceptor density (cm^{-3}) (N_A) ×10^{15}	10^3	0
11.	Radiative recombination co-efficient (cm^3/s)	10^{-9}	10^{-9}
12.	SRH recombination lifetime of electrons (ns)	15	8
13.	SRH recombination lifetime of electrons (ns)	15	8

change in the absorber thickness (≈25 nm) significantly affects Jsc due to the spatial distribution of photo generated carriers and the finite carrier diffusion length. Thinner layers absorb fewer photons, thereby limiting carrier generation, whereas thicker layers experience enhanced recombination, which reduces carrier collection efficiency. Consequently, an optimal absorber thickness of approximately 300 nm is achieved with a combined effect of photon absorption and their efficient collection. Table IV summarizes the comparison of photo voltaic parameters of the proposed perovskite solar cell with some recently reported works. Zhou et al.[5] investigated an FTO/SnO2/ FAPbI3/T2/Au solar cell and reported a PCE of 26.4%. Subsequently, Tian and co-workers [7] optimized the PCE to 20.2% using an ITO/ PEDOT:PSS/ perovskite /OHPEACl /PCBM /BCP /Ag structure. Bhattarai et al. [8] reported a PCE of 26.3% in 2024 through simulation of an ITO/ZnO /CsSnI3/NiO/Au solar cell. In 2025, Chen et al. [9] simulated an FTO/ PTAA/ perovskite /PCBM /BCP /Ag device and obtained a PCE of 23.9%. Similarly, Zhang and collaborators [10] demonstrated a PCE of 24.5% for an FTO/ PEDOT:PSS/ perovskite/C60/BCP/Cu solar cell [9]. In contrast, the proposed ITO/TiO2/CsSnI3 /PEDOT:PSS/Al device in this work achieves a

ISBN: 978-81-985770-0-9

higher PCE of 32.09% with 300 nm thickness of the absorber layer.

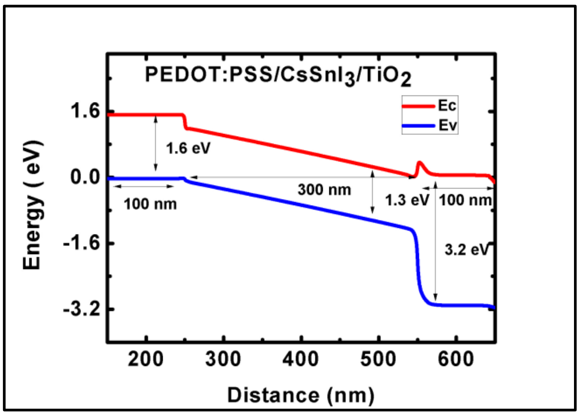

Fig. 4. Energy band diagram of proposed perovskite solar cell derived from CHARGE module.

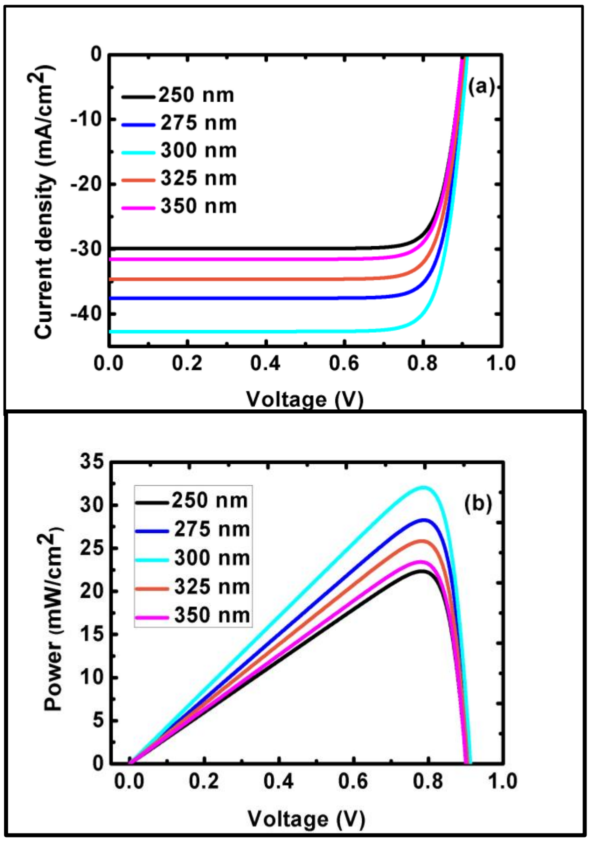

Fig. 5. (a) J-V characteristics and (b) power curve of the proposed PSC for different thickness values of the absorbing layer from 250 nm to 350 nm.

TABLE III
PHOTO-VOLTAIC PARAMETERS OF THE PROPOSED SOLAR CELL WITH DIFFERENT ABSORBER LAYER THICKNESS

Thickness (nm)	Voc (V)	Jsc (mA/cm^2)	FF (%)	PCE (%)
250	0.900	29.90	83.06	22.35
275	0.910	37.57	82.78	28.30
300	0.912	42.71	82.38	32.10
325	0.904	34.64	82.49	25.86
350	0.900	31.55	82.46	23.42

TABLE IV
COMPARISON OF PHOTO-VOLTAIC PARAMETERS OF THE PROPOSED DEVICE WITH RECENTLY REPORTED WORKS

Sl No	Device Structure	J_{sc} (mA/cm^2)	V_{oc} (V)	FF (%)	PCE (%)
1.	FTO/SnO_2/$FAPbI_3$/T2/Au (experimental) [5]	26.47	1.17	84.9	26.4
2.	ITO/PEDOT: PSS/ perovskite/ OHPEACl/PCBM/ BCP/Ag (experimental) [7]	30.37	0.84	79.2	20.2
3.	ITO/ZnO/$CsSnI_3$/NiO /Au (simulated) [8]	32.44	1.02	79.5	26.3
4.	FTO/PTAA/ perovskite/ PCBM/BCP/Ag (simulated) [9]	32.98	0.88	81.8	23.9
5.	FTO/PEDOT: PSS/perovskite/ C60/BCP/Cu (simulated) [10]	33.55	0.89	81.6	24.5
6.	ITO/TiO_2/$CsSnI_3$/PEDOT:PSS/Al (This work)	42.71	0.91	82.4	32.1

V. CONCLUSION

The photovoltaic performance of the ITO/TiO_2/$CsSnI_3$/ PEDOT:PSS/Al solar cell has been systematically investigated using ANSYS Lumerical. $CsSnI_3$, being a lead-free and eco-friendly alternative to conventional lead-based perovskites with a narrow bandgap, effectively captures a broad portion of the solar spectrum, thereby enhancing the power conversion efficiency. Furthermore, the favorable band alignment among the constituent layers facilitates efficient carrier extraction while suppressing the backflow of electrons and holes, which reduces recombination losses at the ETL–HTL interfaces. Through thickness optimization and appropriate selection of ETL and HTL materials, a

ISBN: 978-81-985770-0-9

300 nm absorber layer yields optimal performance with a maximum J_{sc} of 42.71 mA/cm², Voc of 0.91 V, FF of 82.4%, and a PCE of 32.1%. The optimized structure demonstrates improved photo-conversion efficiency compared with previously reported designs, emphasizing the potential of the proposed architecture for high-efficiency, environmentally benign perovskite solar cells.

Future research will focus on fabrication and characterization of the proposed device under varying environmental conditions, with further optimization to improve the device efficiency in long term.

ACKNOWLEDGEMENT

The authors acknowledge the financial support provided by RUSA 2.0, CenSISA, Area-3, University of Calcutta, which facilitated the successful completion of this research work.

REFERENCES

[1] S. Bankura and A. Biswas, "Optimized integration of shape-tailored metallic nanostructure for performance enhancement in all inorganic perovskite solar cells," Journal of Physics and Chemistry of Solids, vol. 207, 112942, 2024. https://doi.org/10.1016/j.jpcs.2025.112942

[2] Z. Iqbal, F. Zu, A. Mussikeno, E. Gutierrez-Patrida, H. Kobler, T. W. Gries, G. V. Sannino, L. Canil, N. Koch, M. Pavone, A.B. Munoz-Garcia, A. Abate, Q. Wang, "Interface modification for energy level alignment and charge extraction in $CsPbI_3$ perovskite solar cells", ACS Energy Lett., vol. 8., pp 4304-4314, 2023. https://doi.org/10.1021/acsenergylett.3c01522

[3] N. Bala and S.K. Mallik, "Investigating Effect of Various ETL and HTL on the Solar Cell Parameters of $CsSn_{0.5}Ge_{0.5}I_3$ based lead Free PsC to Obtain Optimized PCE," Indian Journal of Pure & Applied Physics, vol. 62, pp. 789–805, 2024. https://doi.org/10.56042/ijpap.v62i9.11102

[4] Q. Fatima, A. A. Haidry, R. Hussain, H. Zhang, "Device Simulation of a Thin-Layer $CsSnI_3$-Based Solar Cell with Enhanced 31.09% Efficiency," Energy Fuels, vol. 37, pp. 7411-7432, 2023. https://doi.org/10.1021/acs.energyfuels.3c00645

[5] J. Zhou, L. Tan, Y. Liu, H. Li, X. Liu, M. Li, S. Wang, Y. Zhang, C. Jiang, R. Hua, W. Tress, S. Meloni, C. Yi, "Highly efficient and Stable perovskite solar cells via a multifunctional hole trasport material," Joule, vol. 8, pp 1691-1706, 2024. https://doi.org/10.1016/j.joule.2024.02.019

[6] S Bankura and A. Biswas, " Analytical Model of All-Inorganic 2-D Ruddlesden–Popper (RP) Layered Halide Perovskite Solar Cells and Their Performance Optimization", IEEE Transaction on Electron Device, vol. 7, no. 16, 2024. https://doi.org/10.1109/TED.2024.3394450

[7] C. Tian, Z. Zhang, A. Sun, J. Liang, Y. Zheng, X. Wu, Y. Liu, C. Tang, C. C. Chen, "Tuning phase stability and interfacial dipole for efficient methylammonium- free Sn-Pb perovskite solar cells," Nano Energy, vol. 116, 108838, 2023. https://doi.org/10.1016/j.nanoen.2023.108848

[8] S. Bhattarai, "Designing a more efficient $CsSnI_3$ based perovskite solar cell with novel bio-synthesized ZnO-NP as ETL," Materials Chemistry and Physics, vol 318, Art. No. 129040, 2024. https://doi.org/10.1016/j.matchemphys.2024.129269

[9] J. Chen, J. Du, J. Cai, B. Ouyang, Z. Li, X. Wu, C. Tian, A. Sun, R. Zhuang, X. Wu, C. Chen, T. Cen, R. Li, T. Xue, Y. Zhao, K. Zhao, Q. Chen, C.-C. Chen, "Lewis Base Strategy for Crystallization Control and Buried Interface Passivation on Hydrophobic PTAA Substrate for Efficient Tin–Lead Perovskite and All-Perovskite Tandem Solar Cells," ACS Energy Lett., Vol. 10, pp. 1117–1128, 2025. https://doi.org/10.1021/acsenergylett.4c03370

[10] Y. Zhang, C. Li, H. Zhao, Z. Yu, X. Tang, J. Zhang, Z. Chen, J. Zeng, P. Zhang, L. Han, H. Chen, "Synchronized crystallization in Tin–Lead perovskite solar cells," Nat. Commun., vol 15, Art. No. 6887, 2024. https://doi.org/10.1038/s41467-024-51361-2

[11] S. Bankura and A. Biswas, " Optimization of lead-free all-inorganic two-dimensional $Cs_3Sb_2I_9$ based perovskite solar cell utilizing diverse charge transport layers and its temperature-dependent performance", Physics Scripta, vol. 100, 085535, 2025. https://jglobal.jst.go.jp/en/public/202502285958899345

[12] P. Nath and A. Biswas, "Engineering the Absorber Architecture for High-Efficiency Lead-Free Inorganic Perovskite Solar Cells in a Trilayer Two-Terminal Design", Physics Status Solidi A, vol. 223, e202500849, 2025. https://doi.org/10.1002/pssa.202500489

[13] J. Park, K. M. Griffith, and Y. Duan, "Systematic Characterization on Optical and Phonon Properties of $Cs[Pb_xSn_{1-x}]I_3$ Alloyed Perovskites via First-Principles Modeling," *Journal of Physical Chemistry C*, vol. 122, no. 50, pp. 29132–29139, 2018. https://doi.org/10.1021/acs.jpcc.2c00797

[14] S. Gedey, "Introduction to the Finite-Difference Time-Domain (FDTD) Method for Electromagnetics," Springer Nature, 2022. https://doi.org/10.1007/978-3-031-01712-4

[15] K. Matsuzawa, K. Uchida, A. Nishiyama, "Unified simulation of Schottky and Ohmic contacts," *IEEE Transactions on Electron Devices*, vol. 47, pp. 881–888, 2000. https://doi.org/10.1109/16.817574

ISBN: 978-81-985770-0-9

[16] Y.Bougdid, G.Kulkarni, F. Chenard, C.J.Sugrim, R.Kumar, A. Kar, “Optical Properties of transparent TiO_2 films by sintering anatase nanoparticle with a CO_2 laser”, Optical Materials, vol. 156, **Art. no. 115276, 2024.** https://doi.org/10.1016/j.optmat.2024.115969

Cite this article as:

Nabanita Mondal , Abhijit Biswas and et. al. 32% Efficient Thickness Optimized Lead-Free CsSnI3 Perovskite Solar Cells with TiO2 Electron Transport Layer", Proceedings of 13th international conference on Microelectronics, Circuits and Systems, Micro2026

Displayed as online on 08th July 2026.

Link: http://actsoft.org/science/micro2026-pro/320-micro2026.pdf

ISBN: 978-81-985770-0-9